The Astrophysical Journal Letters, 758:L23 (6pp), 2012 October 10 doi:10.1088/2041-8205/758/1/L23
© 2012. The American Astronomical Society. All rights reserved. Printed in the U.S.A.

CONSTRAINTS ON THE SHAPE OF THE MILKY WAY DARK MATTER HALO FROM JEANS EQUATIONS APPLIED TO SLOAN DIGITAL SKY SURVEY DATA

Sarah R. Loebman[1], Željko Ivezić[1], Thomas R. Quinn[1], Fabio Governato[1], Alyson M. Brooks[2,5], Charlotte R. Christensen[3,6], and Mario Jurić[4]
[1] Astronomy Department, University of Washington, Box 351580, Seattle, WA 98195-1580, USA; sloebman@astro.washington.edu
[2] Department of Astronomy, University of Wisconsin, 475 North Charter Street, Madison, WI 53706, USA
[3] Astronomy Department, University of Arizona, Tucson, AZ, USA
[4] LSST Corporation, 933 North Cherry Avenue, Tucson, AZ 85721, USA
Received 2012 July 13; accepted 2012 September 12; published 2012 September 26

ABSTRACT

We search for evidence of dark matter in the Milky Way by utilizing the stellar number density distribution and kinematics measured by the Sloan Digital Sky Survey (SDSS) to heliocentric distances exceeding ∼10 kpc. We employ the cylindrically symmetric form of Jeans equations and focus on the morphology of the resulting acceleration maps, rather than the normalization of the total mass as done in previous, mostly local, studies. Jeans equations are first applied to a mock catalog based on a cosmologically derived *N*-body + SPH simulation, and the known acceleration (gradient of gravitational potential) is successfully recovered. The same simulation is also used to quantify the impact of dark matter on the total acceleration. We use Galfast, a code designed to quantitatively reproduce SDSS measurements and selection effects, to generate a synthetic stellar catalog. We apply Jeans equations to this catalog and produce two-dimensional maps of stellar acceleration. These maps reveal that in a Newtonian framework, the implied gravitational potential cannot be explained by visible matter alone. The acceleration experienced by stars at galactocentric distances of ∼20 kpc is three times larger than what can be explained by purely visible matter. The application of an analytic method for estimating the dark matter halo axis ratio to SDSS data implies an oblate halo with $q_{\rm DM} = 0.47 \pm 0.14$ within the same distance range. These techniques can be used to map the dark matter halo to much larger distances from the Galactic center using upcoming deep optical surveys, such as LSST.

Key words: Galaxy: general – Galaxy: halo – Galaxy: kinematics and dynamics – Galaxy: structure – stars: kinematics and dynamics – stars: statistics

Online-only material: color figures

1. INTRODUCTION

Determining the dark matter content of the Milky Way has important implications for fields ranging from theories of galaxy formation and evolution to experimental physics. Lately, there has been renewed interest in an old concept—applying Jeans equations to stars in the Milky Way to infer the underlying mass distribution (Jeans 1915; Oort 1932). This technique statistically estimates the gravitational potential using observable stellar kinematics, rather than accelerations that are rarely detectable.

Jeans equations follow from the collisionless Boltzmann equation; for a detailed derivation see Binney & Tremaine (1987). Using cylindrical coordinates and assuming an axisymmetric and steady-state system, the accelerations in the radial (R) and vertical (Z) directions can be expressed in terms of observable quantities: the stellar number density distribution ν, the mean azimuthal (rotational) velocity $\overline{v_\phi}$, and four velocity dispersions $\sigma_{\phi\phi}$, σ_{RR}, σ_{ZZ}, and σ_{RZ} (all as functions of R and Z), as

$$a_R = \sigma_{RR}^2 \times \frac{\partial(\ln \nu)}{\partial R} + \frac{\partial \sigma_{RR}^2}{\partial R} + \sigma_{RZ}^2 \times \frac{\partial(\ln \nu)}{\partial Z} + \frac{\partial \sigma_{RZ}^2}{\partial Z} + \frac{\sigma_{RR}^2}{R} - \frac{\sigma_{\phi\phi}^2}{R} - \frac{\overline{v_\phi}^2}{R}, \quad (1)$$

$$a_Z = \sigma_{RZ}^2 \times \frac{\partial(\ln \nu)}{\partial R} + \frac{\partial \sigma_{RZ}^2}{\partial R} + \sigma_{ZZ}^2 \times \frac{\partial(\ln \nu)}{\partial Z} + \frac{\partial \sigma_{ZZ}^2}{\partial Z} + \frac{\sigma_{RZ}^2}{R}. \quad (2)$$

Given accelerations $a_R(R, Z)$ and $a_Z(R, Z)$, i.e., the gradient of the gravitational potential, the dark matter contribution can be estimated after accounting for the contribution from visible matter.

Traditionally, such studies were limited by data to the solar neighborhood (within ∼150 pc; e.g., Kapteyn 1922; Oort 1960; Bahcall 1984). The main conclusion drawn from such local studies is that dark matter contributes a small (of the order 10%) but significantly detected fraction of mass in the solar neighborhood (corresponding to about 0.01 $M_\odot$ pc^{-3}, or 0.38 GeV cm^{-3}; Kuijken & Gilmore 1989; Creze et al. 1998; Holmberg & Flynn 2000).

Several groups have extended these studies to a few kiloparsec from the plane of the disk (Kuijken & Gilmore 1991; Siebert et al. 2003; Holmberg & Flynn 2004; Smith et al. 2012; Bovy et al. 2012). Recently, Garbari et al. (2012) used a sample of 2000 K dwarf stars that extend to 1 kpc above the plane of the disk and estimated the local dark matter density distribution $\rho_{\rm dm} = (0.022 \pm 0.015)\, M_\odot$ pc^{-3}. Using kinematic data for ∼400 thick disk stars at distances of a few kiloparsec from the Galactic plane from Moni Bidin et al. (2012), Bovy & Tremaine (2012) estimated $\rho_{\rm dm} = (0.008 \pm 0.002)\, M_\odot$ pc^{-3}.

[5] Grainger Postdoctoral Fellow.
[6] Theory Fellow.

It has been difficult to extend these measurements to distances beyond a few kiloparsec from the solar neighborhood (van der Marel 1991). Recently, using a sample of ∼2500 blue horizontal branch stars from SDSS DR6, Xue et al. (2008) found an estimate of the Milky Way's circular velocity curve at ∼60 kpc that implied the existence of dark matter. Using a spherical approximation of Jeans equations and extending the analysis of the Xue et al. (2008) sample, Samurović & Lalović (2011) also concluded that the Newtonian model without dark matter cannot fit the observed velocity dispersion profile. They also tested various modified Newtonian dynamics models and concluded that these fit the data as well.

Here, we extend these studies and introduce a novel multi-dimensional application of Jeans equations made possible by the Sloan Digital Sky Survey[7] data (hereafter SDSS; York et al. 2000). Due to substantial SDSS sky coverage and accurate multi-color photometry to faint limits, the stellar number density distribution and stellar kinematics were mapped out using numerous main-sequence stars detected to galactocentric distances of ∼20 kpc (Jurić et al. 2008; Ivezić et al. 2008a; Bond et al. 2010). The extent of these maps is sufficiently large that it is possible to investigate stellar acceleration via Jeans equations. Most importantly, while the spatial derivatives of the velocity dispersion are extremely difficult to constrain from the local solar neighborhood, they can be directly measured using SDSS data. We discuss here the following main questions.

1. How does the inclusion or exclusion of a dark matter component affect the morphology of the stellar acceleration maps?
2. Is it possible to recover the known accelerations by applying Jeans equations to a realistic simulated galaxy that has a merger history and is not perfectly axisymmetric?
3. Are stellar acceleration maps derived from SDSS data consistent with expectations based only on visible matter?

This paper provides a brief summary of our analysis; a detailed discussion will be presented elsewhere (S. R. Loebman et al., in preparation). In Section 2, we describe the simulation employed in this work and answer the first two questions. The main result of this work, an answer to the third question, is presented in Section 3. We summarize and discuss our results in Section 4.

2. TESTING THE METHODOLOGY

2.1. N-body + SPH Simulation

To test the Jeans equation approach, we apply our analysis tools to a simulation with *known* accelerations and velocities. We use a cosmologically derived (WMAP3; Spergel et al. 2003) Milky Way–mass galaxy evolved for 13.7 Gyr using the parallel N-body + SPH code GASOLINE (Wadsley et al. 2004), which contains realistic gas, cooling, and stellar feedback (Stinson et al. 2006; Shen et al. 2009; Christensen et al. 2012). We track the galaxy's formation and evolution using the volume renormalization technique (Katz & White 1993; Pontzen et al. 2008; Governato et al. 2012). Our simulated galaxy includes a stellar halo, which is built up primarily during the merging process in a ΛCDM cosmology (e.g., Bullock & Johnston 2005; Zolotov et al. 2009).

GASOLINE simultaneously calculates the potential and the acceleration that particles feel; force calculations are consistent with other state-of-the-art cosmological gas-dynamical codes (Power et al. 2003; Scannapieco et al. 2012). The typical root-mean-square (rms) acceleration error is ∼0.2% (Wadsley et al. 2004). The average stellar particle mass is ∼5800 $M_\odot$ and the dark matter particle mass is $1.3 \times 10^5\ M_\odot$, with a dark matter softening length of 173 pc. At a redshift of zero, the simulated galaxy has a virial radius, defined at $\rho/\rho_{\rm crit} = 100$, of 227 kpc (versus the Milky Way's 200 kpc; see Boylan-Kolchin et al. 2011) and a virial mass of $7 \times 10^{11}\ M_\odot$ (versus the Milky Way's $1.0^{+0.3}_{-0.2} \times 10^{12}\ M_\odot$; see Xue et al. 2008; Klypin et al. 2002), of this, 7% is in gas, 6% is in stars, and 87% is in dark matter. Dark matter consists of 36% of the total mass in the region corresponding to the solar neighborhood ($7 \leqslant R/{\rm kpc} \leqslant 9$ and $0 \leqslant Z/{\rm kpc} \leqslant 1$). The simulated galaxy is approximately rotationally symmetric (a total matter axis ratio $b : a > 0.9$ within 100 kpc, and a stellar matter axis ratio $b : a > 0.95$ at $R = 10$ kpc), has an R-band disk scale length of ∼3.1 kpc (versus the Milky Way's 3.6 kpc; see Jurić et al. 2008) and corresponding bulge to disk ratio of 0.33 (Jonsson 2006), and the circular velocity at 2.2 disk scale lengths is ∼208 km s^{-1} (versus the Milky Way's 220 km s^{-1}; see Xue et al. 2008). We draw direct comparisons between the simulation and the Milky Way as these structural parameters are within 15% of one another.

For the sake of brevity, we focus our presentation on the acceleration in the Z-direction, a_Z; detailed analysis of the acceleration in the R-direction, a_R, will be presented in a subsequent paper. The top panel of Figure 1 shows a_Z within the simulation. For comparison, the middle panel shows an analogous map when only contributions from star and gas particles are included. As is evident, there are substantial differences in the morphology of the two maps; the bottom panel demonstrates that the effect of dark matter on the resulting acceleration increases quickly toward the outer parts of the galaxy; for example, the ratio of accelerations is doubled by $R = 8$ kpc and $Z = 6$ kpc. These distances are probed by SDSS—hence our results suggest that the effect of dark matter on stellar acceleration may be uncovered in SDSS data.

2.2. Application of Jeans Equations to the Simulation

Here, we verify that the known gravitational accelerations in the simulation can be recovered using Jeans equations. We bin the star particles into 1 kpc × 1 kpc rectilinear pixels in R–Z space and limit our analysis to bins containing at least 100 star particles. Using weights proportional to the mass of each star particle, we create maps of $\ln(\nu)$ and kinematic quantities. The spatial derivatives of these quantities at the position of each pixel are computed by first fitting a second-order polynomial in R and Z using the eight neighboring pixels, and then taking derivatives analytically; edge pixels are discarded to minimize the impact of fitting errors.

We compare the acceleration in the Z-direction computed using Equations (1) and (2) to the true acceleration in Figure 2. The recovered acceleration map is close to the true map: The distribution of pixel values from the bottom panel is centered on 1.05 with an rms of 0.24. Similar agreement is obtained for the acceleration in the R-direction, which is centered on 1.02 with an rms value of 0.38.

We note that Jeans equations recover meaningful acceleration maps even though the simulation is neither perfectly rotationally symmetric nor steady state. Given this precedence, we apply the same technique to synthetic SDSS data.

[7] www.sdss.org

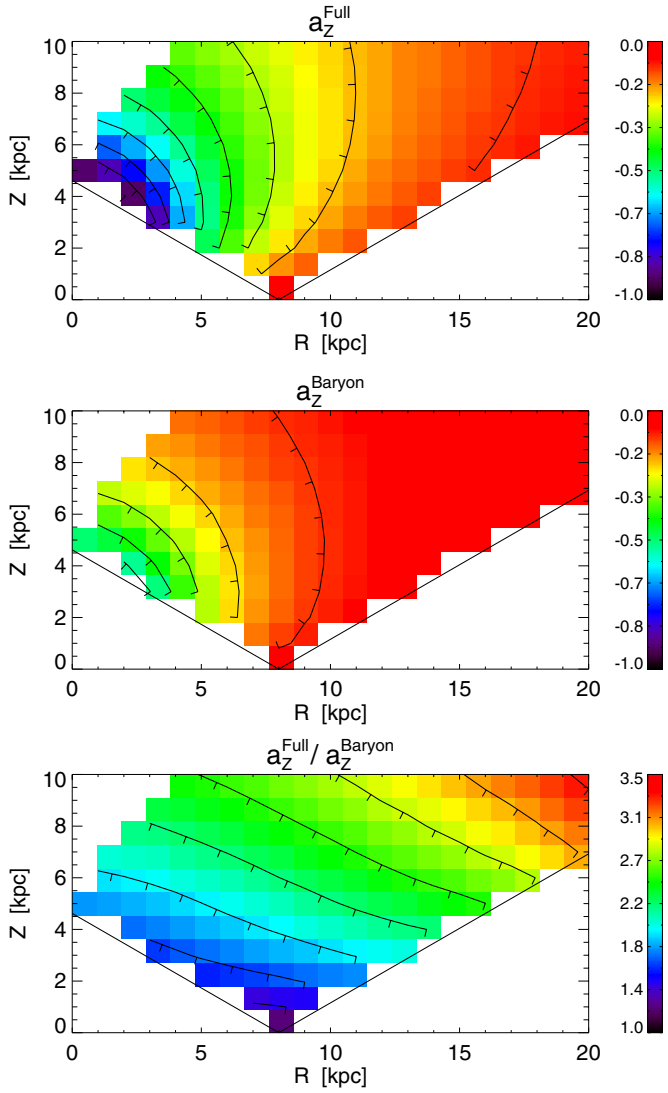

Figure 1. Comparison of the acceleration in the Z-direction when all contributions are included (star, gas, and dark matter particles; top panel) to the result without dark matter (middle panel). The acceleration is expressed in units of 2.9×10^{-13} km s^{-2}. The ratio of the two maps is shown in the bottom panel. The importance of the dark matter increases with the distance from the origin; at the edge of the volume probed by SDSS ($R \sim 20$ kpc, $Z \sim 10$ kpc), the total acceleration in the analyzed simulation is about three times larger than the contribution from the visible matter. The maps are limited to the volume explored by SDSS data, as indicated by the diagonal lines encapsulating the colored pixels.

(A color version of this figure is available in the online journal.)

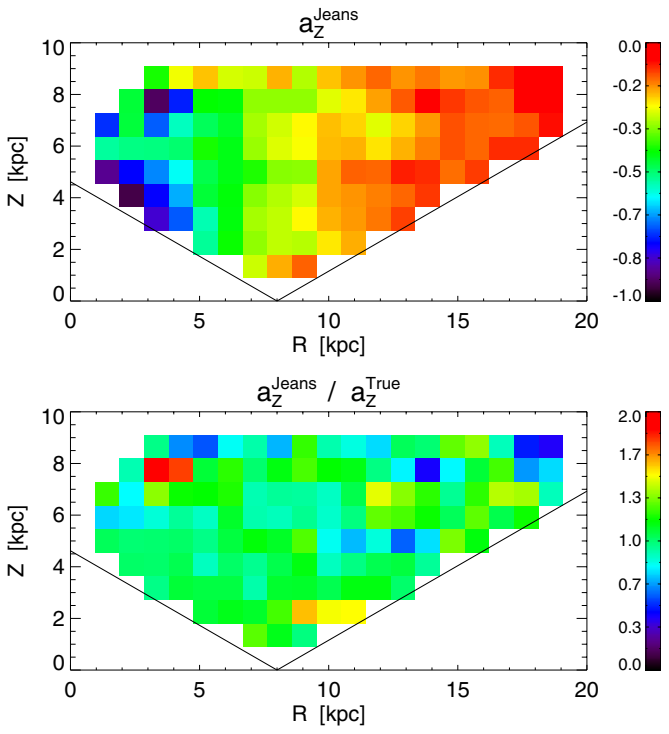

Figure 2. Top panel: the acceleration in the Z-direction derived using Equation (2) and expressed in units of 2.9×10^{-13} km s^{-2}. Bottom panel: the ratio of the top panel to the true acceleration in the Z-direction (top panel of Figure 1).

(A color version of this figure is available in the online journal.)

3. RESULTS

A direct application of Jeans equations to SDSS data would be complicated because of the complex selection effects and the impact of substructure. Instead, we employ a catalog generated using the code Galfast, which is designed to quantitatively reproduce the SDSS measurements, volume coverage, selection, and other instrumental effects. It incorporates smooth models for the stellar number density distribution, metallicity distribution, and kinematics based on tomographic analysis of SDSS data (Jurić et al. 2008; Ivezić et al. 2008a; Bond et al. 2010). The most important ingredients for this study are the best-fit power-law halo given by Equation (24) in Jurić et al. (2008), with power-law index $n_H = 2.77 \pm 0.2$, axis ratio $q_H = 0.64 \pm 0.1$, and halo velocity ellipsoid that is invariant in spherical coordinates (Bond et al. 2010), with $\sigma_r = 141$ km s^{-1}, $\sigma_\theta = 75$ km s^{-1}, and $\sigma_\phi = 85$ km s^{-1}. While the same analytic models could be used to directly generate acceleration maps, we use mock catalogs instead to account for shot noise due to a finite number of stars and edge effects and to ensure that the same analysis code verified on the simulation is used when processing real data. We emphasize that the cylindrical symmetry built into Galfast is fully consistent with SDSS data (after local substructure is masked; see Jurić et al. 2008).

Using Galfast, we generate a flux-limited catalog with $14 < r < 21$ and mimic the SDSS sky footprint by only considering high Galactic latitudes ($|b| > 30°$). A halo-like sample of 0.61 million stars is selected using $M_r \geqslant 4$ and $0.25 < g - r < 0.35$. This sample is dominated by low-metallicity main-sequence F stars. The catalog lists true positions, absolute magnitudes, velocities, and metallicity, as well as corresponding simulated SDSS observations convolved with measurement errors.

Figure 3 shows the three observables constructed using the Galfast catalog that are required to compute a_Z using Equation (2). As expected, both velocity dispersions are smoothly varying, and the σ_{RZ}^2 is at most 40% of the maximal σ_{ZZ}^2 value.

The top panel of Figure 4 shows the resulting a_Z map. The middle and bottom panels show the ratio of this map compared to the simulation data in the two maps shown in the top and middle panels in Figure 1. It is evident that the acceleration map implied by SDSS data is much closer to the model-based acceleration map that includes contributions from both baryons and dark matter. When dark matter is not included, the model-based map has a different shape than the map derived from SDSS data: It underpredicts the observed acceleration by roughly a

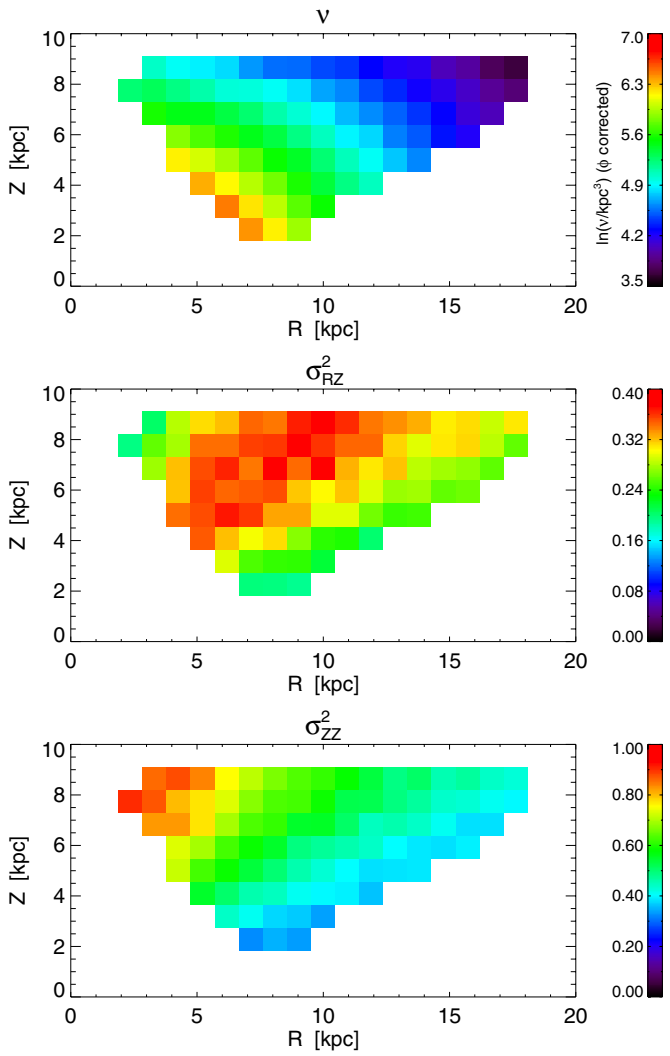

Figure 3. Three observables as implied by SDSS data (number density distribution in the top panel, and the two velocity dispersions in the other panels, as marked, both expressed in units of 2×10^4 (km s^{-1})^2) that are required to compute $a_Z(R, Z)$ using Equation (2). The pixels at $Z < 1$ kpc are unreliable due to SDSS saturation at $r = 14$; additionally, we restrict our fits to regions with eight adjacent pixels.

(A color version of this figure is available in the online journal.)

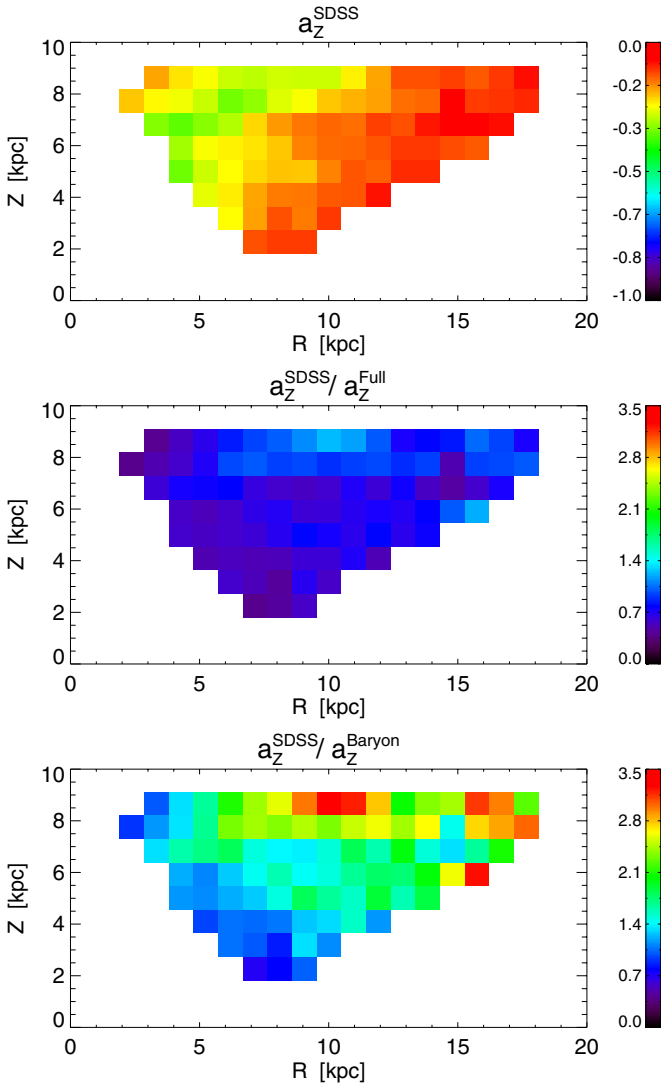

Figure 4. Results of applying Jeans equations to the SDSS observations simulated using Galfast. The top panel shows a map of the acceleration in the Z-direction expressed in units of 2.9×10^{-13} km s^{-2}. The middle and bottom panels show the ratio of the map from the top panel and the two model-based maps shown in the top two panels in Figure 1.

(A color version of this figure is available in the online journal.)

factor of three at $R \sim 17$ kpc and $Z \sim 9$ kpc. A pixel-by-pixel comparison of the two ratio maps is shown in the top panel in Figure 5; the fact that the *shape* of the observed acceleration map is better matched when dark matter is included is seen in the much narrower histogram. These results are not unique to a_Z; the bottom panel in Figure 5 shows the same result for a_R, with even larger deviations between the observed map and the model-based map that does not include dark matter contribution.

Our preliminary analysis of other simulations indicates that the observed acceleration map cannot be reproduced by simply increasing the amount of baryons and not including dark matter: the key difficulty is to reproduce the strong acceleration at 10–20 kpc from the Galactic center while simultaneously maintaining the shape of the acceleration map throughout the probed volume.

4. DISCUSSION AND CONCLUSIONS

We have shown that the kinematics of stars can be used to probe the dark matter distribution in the Milky Way. To do so, we used a cosmologically derived N-body+SPH Milky-Way-like simulation to demonstrate that Jeans equations are capable of recovering the underlying gravitational potential despite small deviations from an implied steady-state axisymmetric system. The same simulation was also used to estimate the dark matter contribution to the resulting acceleration maps.

We also generated a synthetic SDSS catalog using Galfast, a code designed to quantitatively reproduce measurements of spatial density and kinematics of Milky Way stars, as well as SDSS volume coverage, selection, and other instrumental effects. With this catalog, we created acceleration maps using Jeans equations. The morphology of these maps provides strong evidence for the presence of dark matter. This evidence is not sensitive to the overall dark matter to baryon mass ratio (that is, the *normalization* of the acceleration maps), which can be considered as a fine-tuning model parameter, but is robustly derived from the *shape* of observed acceleration maps.

While the method presented here does not yet provide errors for the total estimate of dark matter in the Milky Way, it

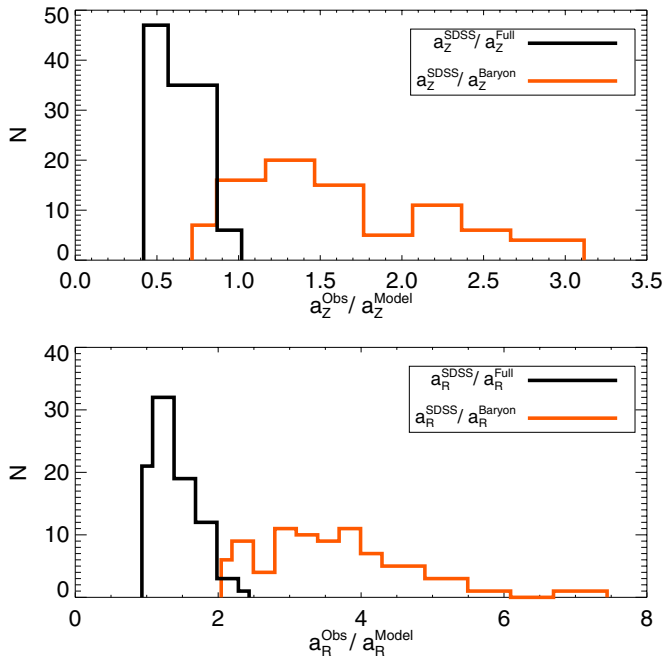

Figure 5. Pixel-by-pixel comparison of the acceleration values implied by the SDSS data and the two model predictions that include (black lines) and do not include (red lines) contributions from dark matter. The top panel corresponds to the a_Z acceleration maps shown in Figure 4 and the bottom panel to the a_R acceleration maps. The model-based acceleration maps that include a dark matter contribution provide a significantly better description of the acceleration maps derived from the SDSS data.

(A color version of this figure is available in the online journal.)

does provide an expanded view of the distribution of dark matter beyond the solar neighborhood. Significantly, it allows us to consider how the distribution of dark matter evolves both radially and vertically in the context of a large, observationally motivated data set. Given a large number of simulations with different dark matter halo properties, it will be possible to constrain the overall dark matter to baryonic mass ratio and the shape of the Milky Way's dark matter halo.

Before such a suite of simulations is generated, we can approximately estimate the shape of the dark matter halo using the method proposed by van der Marel (1991). He showed that for an oblate dark matter halo with a density distribution similar to a singular isothermal sphere, it is possible to derive the dark matter axis ratio from the stellar halo axis ratio and the velocity ellipsoid (via application of Jeans equations; see his Equations (1) and (21) and Figure 1). Using SDSS measurements for the stellar halo axis ratio and the velocity ellipsoid (see Section 3), we estimated that the minor to major axis ratio of the Milky Way's dark matter halo is $q_{\rm DM} = 0.47 \pm 0.14$. Compared to the stellar halo axis ratio, $q_H = 0.64 \pm 0.1$, the dark matter halo is more oblate.

The N-body+SPH simulation used in this work supports the properties of the dark matter halo assumed in the van der Marel's method; in particular, its density decrease is consistent with expected $1/[R^2+(Z/q_{\rm DM})^2]$ within 30 kpc from the origin (with the power-law index decreasing from -2 to about -2.8 at larger distances). At the same time, the stellar halo is consistent with $n_H = 2.77$ measured by SDSS in the same distance range. While it is premature to declare $q_{\rm DM} = 0.47 \pm 0.14$ as a robust measurement of the dark matter halo shape, it is encouraging that the simulation is at least qualitatively consistent with SDSS data in so many aspects.

Moreover, it is possible to go beyond Jeans equations to use stellar kinematics to probe the full phase space distribution of stars. As Valluri et al. (2012) demonstrated, orbital spectral analysis can be used to determine not only the shape of the inner halo, but the global shape of the Galactic halo as well. Their technique provides a complementary tool to the method presented here for constraining the potential and the stellar distribution function.

We note, there is a considerable range of Milky Way dark matter halo axis ratios presented in the literature. The reported axis ratio ranges from >0.7 at the low end (Ibata et al. 2001) to 5/3 at the high end (Helmi 2004). Sometimes, triaxial models are incorporated, such as by Law & Majewski (2010) who used observations of the Sgr tidal stream and N-body modeling to conclude that the Milky Way has a triaxial dark matter halo that is nearly an oblate ellipsoid whose minor axis is contained within the Galactic disk plane. Lux et al. (2012) used satellite galaxies to find that the Milky Way dark matter halo is oblate, while Banerjee & Jog (2011) used observations of H I and claimed variation of the axis ratio, with the halo increasingly prolate at large distances.

The full promise of various methods for estimating the geometry of dark matter halos will be reached by upcoming next-generation surveys, such as *Gaia* (Perryman 2002) and LSST (Ivezić et al. 2008b). *Gaia* will provide measurements of geometric distances and kinematics with a similar faint flux limit as SDSS, but with much smaller errors. LSST will obtain photometric distances and kinematics of comparable accuracy to those of *Gaia* at *Gaia*'s faint limit, but extend them deeper by about 5 mag. With LSST and *Gaia*, it will be possible to extend Galactic potential studies such as the one presented here to distances roughly 10 times larger than those possible with SDSS data, revolutionizing our understanding of the Milky Way in the process.

S.L. and Ž.I. acknowledge support by NSF grants AST-0707901 and AST-1008784 to the University of Washington, by NSF grant AST-0551161 to LSST for design and development activity, and by the Croatian National Science Foundation grant O-1548-2009. Resources supporting this work were provided by the NASA High-End Computing (HEC) Program through the NASA Advanced Supercomputing (NAS) Division at Ames Research Center. Galfast computations were performed on Hybrid at the Physics Department, University of Split, financed by the National Foundation for Science, Higher Education and Technological Development of the Republic of Croatia. F.G. acknowledges support from NSF grant AST-1108885; A.B. acknowledges support from the Grainger Foundation. S.L. acknowledges support from the Washington NASA Space Grant Consortium.

REFERENCES

Bahcall, J. N. 1984, ApJ, 276, 169
Banerjee, A., & Jog, C. J. 2011, ApJ, 732, L8
Binney, J., & Tremaine, S. 1987, Galactic Dynamics (Princeton, NJ: Princeton Univ. Press)
Bond, N. A., Ivezić, Ž., Sesar, B., et al. 2010, ApJ, 716, 1
Bovy, J., Rix, H.-W., & Hogg, D. W. 2012, ApJ, 751, 131
Bovy, J., & Tremaine, S. 2012, ApJ, 756, 89
Boylan-Kolchin, M., Besla, G., & Hernquist, L. 2011, MNRAS, 414, 1560
Bullock, J. S., & Johnston, K. V. 2005, ApJ, 635, 931
Christensen, C., Quinn, T., Governato, F., et al. 2012, MNRAS, 425, 3058
Creze, M., Chereul, E., Bienayme, O., & Pichon, C. 1998, A&A, 329, 920
Garbari, S., Liu, C., Read, J. I., & Lake, G. 2012, MNRAS, 425, 1445

Governato, F., Zolotov, A., Pontzen, A., et al. 2012, MNRAS, 422, 1231
Helmi, A. 2004, ApJ, 610, L97
Holmberg, J., & Flynn, C. 2000, MNRAS, 313, 209
Holmberg, J., & Flynn, C. 2004, MNRAS, 352, 440
Ibata, R., Lewis, G. F., Irwin, M., Totten, E., & Quinn, T. 2001, ApJ, 551, 294
Ivezić, Ž., Sesar, B., Jurić, M., et al. 2008a, ApJ, 684, 287
Ivezić, Ž., Tyson, J. A., Acosta, E., et al. 2008b, arXiv:0805.2366
Jeans, J. H. 1915, MNRAS, 76, 70
Jonsson, P. 2006, MNRAS, 372, 2
Jurić, M., Ivezić, Ž., Brooks, A., et al. 2008, ApJ, 673, 864
Kapteyn, J. C. 1922, ApJ, 55, 302
Katz, N., & White, S. D. M. 1993, ApJ, 412, 455
Klypin, A., Zhao, H., & Somerville, R. S. 2002, ApJ, 573, 597
Kuijken, K., & Gilmore, G. 1989, MNRAS, 239, 651
Kuijken, K., & Gilmore, G. 1991, ApJ, 367, L9
Law, D. R., & Majewski, S. R. 2010, ApJ, 714, 229
Lux, H., Read, J. I., Lake, G., & Johnston, K. V. 2012, MNRAS, 424, L16
Moni Bidin, C., Carraro, G., Mendez, R. A., & Smith, R. 2012, ApJ, 751, 30
Oort, J. H. 1932, Bull. Astron. Inst. Neth., 6, 249
Oort, J. H. 1960, Bull. Astron. Inst. Neth., 15, 45
Perryman, M. A. C. 2002, Ap&SS, 280, 1
Pontzen, A., Governato, F., Pettini, M., et al. 2008, MNRAS, 390, 1349
Power, C., Navarro, J. F., Jenkins, A., et al. 2003, MNRAS, 338, 14
Samurović, S., & Lalović, A. 2011, A&A, 531, A82
Scannapieco, C., Wadepuhl, M., Parry, O. H., et al. 2012, MNRAS, 423, 1726
Shen, S., Wadsley, J., & Stinson, G. 2009, arXiv:0910.5956
Siebert, A., Bienaymé, O., & Soubiran, C. 2003, A&A, 399, 531
Smith, M. C., Whiteoak, S. H., & Evans, N. W. 2012, ApJ, 746, 181
Spergel, D. N., Verde, L., Peiris, H. V., et al. 2003, ApJS, 148, 175
Stinson, G., Seth, A., Katz, N., et al. 2006, MNRAS, 373, 1074
Valluri, M., Debattista, V. P., Quinn, T. R., Roškar, R., & Wadsley, J. 2012, MNRAS, 419, 1951
van der Marel, R. P. 1991, MNRAS, 248, 515
Wadsley, J. W., Stadel, J., & Quinn, T. 2004, New Astron., 9, 137
Xue, X. X., Rix, H. W., Zhao, G., et al. 2008, ApJ, 684, 1143
York, D. G., Adelman, J., Anderson, J. E., Jr., et al. 2000, AJ, 120, 1579
Zolotov, A., Willman, B., Brooks, A. M., et al. 2009, ApJ, 702, 1058